

# Black hole in the West Nucleus of Arp 220

D. Downes<sup>1</sup> and A. Eckart<sup>2,3</sup>

<sup>1</sup> Institut de Radio Astronomie Millimétrique, Domaine Universitaire, 38406 St-Martin-d'Hères, France

<sup>2</sup> I. Physikalisches Institut, Universität zu Köln, Zulpicherstrasse 77, 50937 Cologne, Germany

<sup>3</sup> Max-Planck-Institut für Radioastronomie, Auf dem Hügel 69, 53121 Bonn, Germany

Received 15 February 2007 / Accepted 13 March 2007

**Abstract.** We present new observations with the IRAM Interferometer, in its longest-baseline configuration, of the CO(2–1) line and the 1.3 mm dust radiation from the Arp 220 nuclear region. The dust source in the West nucleus has a size of  $0.19'' \times 0.13''$  and a 1.3 mm brightness temperature of 90 K. This implies that the dust ring in the West nucleus has a high opacity, with  $\tau = 1$  at 1.1 mm. Not only is the dust ring itself optically thick in the submm and far-IR, but it is surrounded by the previously-known, rapidly rotating molecular disk of size  $0.5''$  that is also optically thick in the mid-IR. The molecular ring is cooler than the hot dust disk because the CO(2–1) line is seen in absorption against the dust disk. The dust ring is massive ( $10^9 M_\odot$ ), compact (radius 35 pc), and hot (true dust temperature 170 K). It resembles rather strikingly the dust ring detected around the quasar APM 08279+52, and is most unlike the warm, extended dust sources in starburst galaxies. Because there is a strong temperature gradient from the hot dust ring to the cooler molecular disk, the heating must come from a concentrated source, an AGN accretion disk that is completely invisible at optical wavelengths, and heavily obscured in hard X-rays.

**Key words.** galaxies: nuclei – galaxies: kinematics and dynamics – galaxies: ISM – galaxies: individual (Arp 220)

## 1. Evidence for a black hole, so far.

Evidence is growing for a supermassive black hole in the West nucleus of the Arp 220 merger:

1) *X-rays*: The *Chandra* point source in the West nucleus has a 2–10 keV luminosity of  $10^7 L_\odot$ , or  $10^{-5}$  times the FIR luminosity. Extended hard X-ray emission in the vicinity raises the total nuclear X-ray luminosity by an order of magnitude, and one cannot rule out a much greater X-ray flux from an AGN hidden behind  $H_2$  column densities  $> 5 \times 10^{24} \text{ cm}^{-2}$  (Clements et al. 2002; Ptak et al. 2003). Updated astrometry yields an even better positional coincidence of the 3–7 keV peak with the West radio nucleus (Iwasawa et al. 2005). The iron  $K\alpha$  emission at 6.7 keV with a large equivalent width (1.9 keV), found by *XMM-Newton*, may also indicate a powerful AGN, hidden by high  $H_2$  column densities (Iwasawa et al. 2005).

2) *Evidence for high column densities that could hide an AGN*: Numerous radio line interferometer maps show a high gas density toward the West nucleus (e.g., Baan & Haschick 1995 (BH95), Scoville et al. 1997; Downes & Solomon 1998 (DS98); Sakamoto et al. 1999; Mundell et al. 2001). High-resolution mid-IR maps from the Keck telescope show a warm dust source in the West nucleus that is opaque at  $25 \mu\text{m}$  (Soifer et al. 1999). On a larger spatial scale than the West nucleus, the global Arp 220 con-

tinuum spectrum measured by the ISO-LWS indicates a dust  $\tau > 1$  at  $100 \mu\text{m}$ , implying an  $H_2$  column density of  $> 2.7 \times 10^{25} \text{ cm}^{-2}$  (Fischer et al. 1997). The OH and  $H_2O$  lines observed by ISO-LWS (González-Alfonso et al. 2004), and the strong deficiency in the PAH  $7.7 \mu\text{m}$  strength vs.  $850 \mu\text{m}$  flux (Haas et al. 2001; Soifer et al. 2002; Spoon et al. 2004) also imply an extinction large enough to hide the hard X-ray emission from an AGN accretion disk.

3) *Plausible cm-VLBI candidates for an AGN* in the West nucleus are the flat-spectrum sources W10, W17, and W42, and the rapidly-varying source W33 (Parra et al. 2007; Lonsdale et al. 2006). VLBA monitoring of the radio supernovae within the Arp 220 nuclei suggest that the supernova rate and starburst efficiency should be revised downward, which would lower the starburst contribution to the total luminosity (Rovilos et al. 2005; but see Lonsdale et al. 2006 and Parra et al. 2007).

4) *Kinematic data*: The CO has a very high velocity spread in the West nucleus. One of the OH masers has a high velocity gradient possibly marking the site of an AGN (Rovilos et al. 2003). Broad ammonia absorption, with a velocity spread of  $700 \text{ km s}^{-1}$ , suggests molecular material in a small, rapidly rotating disk surrounding a black hole (Takano et al. 2005). While the large-scale (15 to 28 kpc) ionized gas is dominated by tidal motions rather than galactic winds (Colina et al. 2004), the complex kinemat-

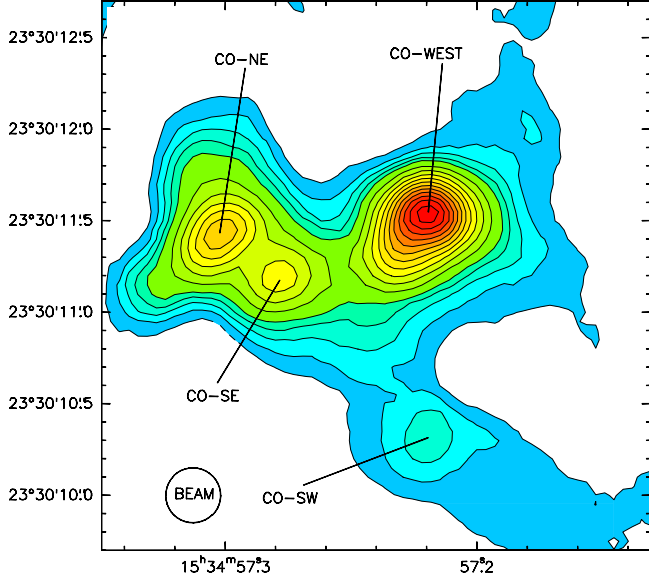


**Fig. 1.** The central 3'' of Arp 220 in CO(2–1) integrated over 770 km s<sup>−1</sup>, with the 1.3 mm continuum subtracted. The beam (*lower left*) is 0.30'' with  $T_b/S = 266$  K/Jy. Contours are 2 to 10 by 2, then 14 to 54 by 4 (in Jy km s<sup>−1</sup>). The CO-West peak is 56.5 Jy km s<sup>−1</sup>; CO-NE is 33.4 Jy km s<sup>−1</sup>.

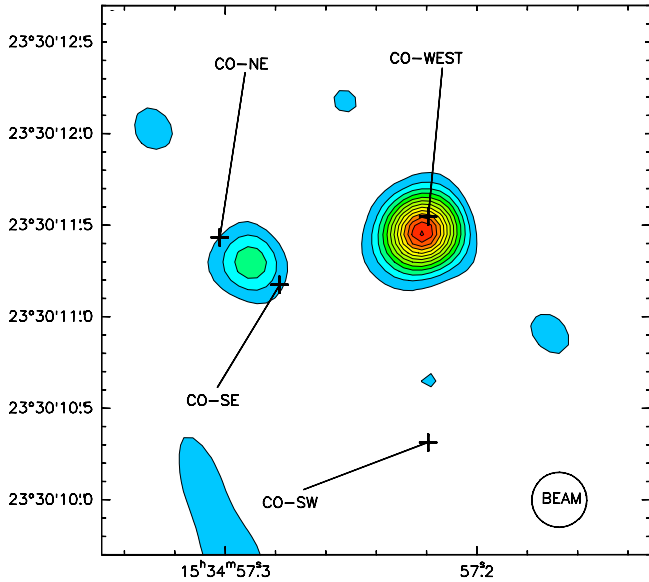


**Fig. 2.** Continuum map at 1.3 mm (229.4 GHz). Contour steps are 6 mJy beam<sup>−1</sup>. The Arp 220-West peak is 79 mJy beam<sup>−1</sup>, and the East peak is 23 mJy beam<sup>−1</sup>. Note that the continuum peaks do not coincide with the CO(2–1) peaks, which are marked with crosses. The beam is 0.30'' (*lower right*).

ics of the ionized gas in the central 2 kpc is influenced by outflows from the dust-enshrouded nucleus — see the H $\alpha$  and [N II] results (Arribas et al. 2001), and the *Chandra* data (McDowell et al. 2003).

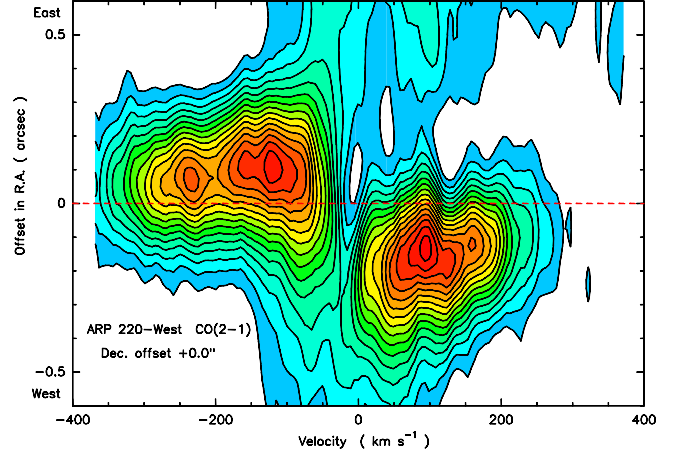


**Fig. 3.** East-west CO(2–1) position-velocity cut, through the West nucleus. CO(2–1) contours are in steps of 10 mJy beam<sup>−1</sup>, with the 1.3 mm continuum subtracted. The CO ring around the West nucleus covers velocities from −370 to +300 km s<sup>−1</sup>, and is cut by absorption at −60 to +40 km s<sup>−1</sup>. Velocity offsets are relative to 226.422 GHz ( $cz_{\text{LSR}} = 5450$  km s<sup>−1</sup>). R.A. offsets are relative to the West continuum peak, indicated by the horizontal line (position in Table 1).

## 2. New long-baseline observations

To further investigate Arp 220’s power source, we re-observed the millimeter continuum and the CO(2–1) and (1–0) lines with the IRAM Plateau de Bure interferometer with its new long baselines to 760 m, which enabled us to restore the data with uniformly-weighted synthesized circular clean beams of 0.30'' at 1.3 mm and 0.60'' at 2.6 mm. We calibrated amplitudes and phases with 3C273, 0923+392, 3C345, and 1502+106. Receiver temperatures were 45 to 65 K at both wavelengths.

This Letter reports on the 1.3 mm results on the West nucleus. We observed the 1.3 mm continuum in the receivers’ upper sideband simultaneously with CO(2–1) in the lower sideband. The spectral correlators covered 770 km s<sup>−1</sup> at 1.3 mm, with a channel spacing of 1.66 km s<sup>−1</sup>. Our velocity scales are relative to 226.422 GHz, which is the rest frequency of CO(2–1) divided by  $1+z_{\text{LSR}}$ , where we took  $cz_{\text{LSR}} = 5450$  km s<sup>−1</sup> as the cosmological redshift. Toward Arp 220,  $V_{\text{LSR}} = V_{\text{hel}} + 16.6$  km s<sup>−1</sup>, so zero velocity offset on our spectra is 5450 km s<sup>−1</sup> (LSR) and 5433 km s<sup>−1</sup> (heliocentric).

The new CO(2–1) map (Fig. 1) shows four peaks, plus an extension of the CO-West gas to the southeast (“source C” on the maps by BH95). The 1.3 mm continuum map (Fig. 2) yields a source position (Table 1) that agrees within the errors with our earlier IRAM data (DS98). But an important new result is the small measured size of the West continuum, which is 0.19''  $\times$  0.13''. This means that the continuum, which at 1.3 mm is mainly dust emission, *does not trace the same matter as the CO(2–1)*. The dust is more compact than the CO emission, which appears to be in a larger ring or disk around the compact dust core.

**Table 1.** Positions, Sizes, and fluxes of the Arp 220-West nuclear disks.

Data	R.A. 15 <sup>h</sup> 34 <sup>m</sup> (J2000)	Dec. 23°30' (J2000)	Major axis (arcsec)	Minor axis (arcsec)	P.A. (deg.)	Observed flux density (mJy)	Model Components Dust (mJy)	H II (mJy)	non-th. (mJy)
<b>Arp 220-West Continuum:</b>									
West 1.3 mm	57 <sup>s</sup> .2226	11.46''	0.19'' ± 0.01''	0.13'' ± 0.02''	−37° ± 6°	106 ± 2	94	10	2.7
West 2.6 mm	57 <sup>s</sup> .2221	11.48''	0.14'' ± 0.08''	—	—	25 ± 1	8.5	11	4.7
<b>West-CO(2–1) −380 to −70 km s<sup>−1</sup>:</b>						(Jy km s <sup>−1</sup> )			
	57 <sup>s</sup> .2265	11.48''	0.37'' ± 0.1''	0.39'' ± 0.1''	−32° ± 5°	74.2	—	—	—
<b>West-CO(2–1) +40 to +380 km s<sup>−1</sup>:</b>									
	57 <sup>s</sup> .2157	11.51''	0.32'' ± 0.1''	0.22'' ± 0.1''	−80° ± 5°	49.3	—	—	—

Estimated position errors are ±0.004<sup>s</sup> in R.A. and ±0.05'' in Dec.

This is clearly shown in the east-west position-velocity cut through the West nucleus (Fig. 3), which covers the full velocity range of 700 km s<sup>−1</sup> in the CO, but with a dramatic change from negative to positive velocities over the central 0.2'', where the CO contours are cut by a deep absorption trough. The CO absorption is even more spectacular in the individual spectra in steps of 0.1'' across the West nucleus (Fig. 4). The main absorption appears to be 100 km s<sup>−1</sup> wide and centered on −10 km s<sup>−1</sup>, with some of the spectra showing a second absorption feature at +130 km s<sup>−1</sup>. Modeling suggests this is partly absorption of the hotter continuum, and CO self-absorption, implying that the CO-West disk itself has a temperature gradient increasing inwards. This is the first time that this Arp 220-West absorption has been seen in CO, and is mainly due to our improved spatial resolution. In previous larger-beam observations, the CO absorption has probably been masked by CO emission in the beam. The CO absorption probably also explains why the West continuum peak is at a slightly different position than the CO (Fig. 2 and Table 1).

### 3. West dust disk: compact, hot and opaque.

The West continuum peak is 79 mJy in our 0.3'' beam, and its spatially integrated flux is 106 mJy, as in our earlier IRAM result (DS98). From lower-frequency data (Sopp & Alexander 1991; Anantharamaiah et al. 2000; Rodriguez-Rico et al. 2005), we estimate that at 1.3 mm, the West nucleus has an extended synchrotron flux of 2.7 mJy, and a free-free continuum of 10 mJy (Table 1; Fig. 5). Extrapolating the 3.6 cm flux of 400 μJy of the variable VLBI source W33 (Parra et al. 2007) with an assumed spectral index of +0.3, as in Sgr A\*, we estimate that any synchrotron self-Compton contribution is < 2 mJy at 1.3 mm. Most of the 1.3 mm flux must therefore be dust emission, at a level of ~ 94 mJy. Hence, the directly-observed, beam-smoothed, dust brightness temperature is 18 K, a remarkably high value at 1.3 mm. Our Gaussian fits to the West continuum in the (*u*, *v*)-plane yield a size of 0.19'' × 0.13'', so the deconvolved dust brightness temperature is a spectacular 90 K at 1.3 mm. The Arp 220 west nucleus is thus a very unusual dust source, not at all like the cooler dust sources detected at millimeter wavelengths in starburst galaxies.

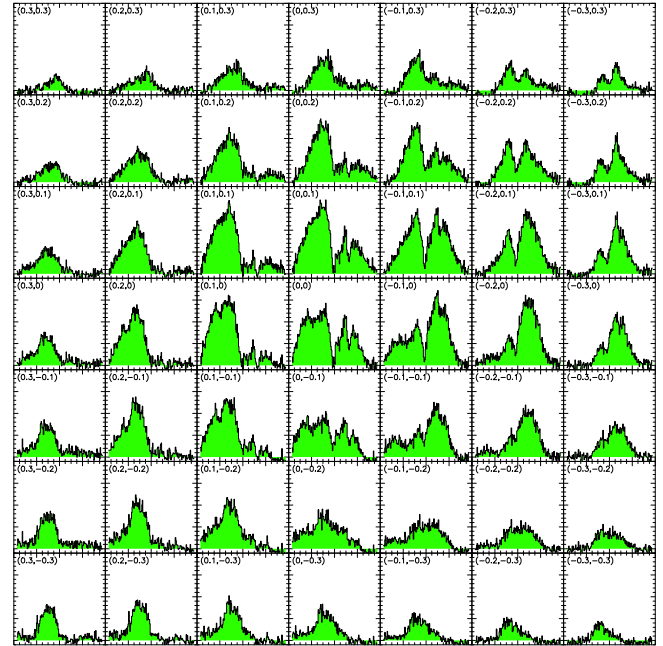


**Fig. 4.** Evidence for foreground obscuration: CO(2–1) spectra across Arp 220-West, with the 1.3 mm continuum subtracted. Each box is a step of 0.1'', north is up, east is left, and (R.A., Dec). offsets are in the upper left of each box. The grid center at (0,0) is the 1.3 mm West continuum peak (Table 1). Velocities run from −400 to +400 km s<sup>−1</sup>, the spectral resolution is 5 km s<sup>−1</sup>, and zero velocity (the center of the spectra) is at 226.422 GHz ( $cz_{\text{lsr}} = 5450$  km s<sup>−1</sup>). Intensities run from 0 to 200 mJy beam<sup>−1</sup>. The beam is 0.30'' with  $T_b/S = 266$  K/Jy, which means the directly-observed, beam-smoothed, peak CO brightness temperatures are 40 K. Note the deep absorption near the line center in some of the spectra, which indicates foreground, cooler gas.

The small source size at 1.3 mm and the deconvolved dust brightness temperature already imply that the 1.3 mm dust opacity is unusually high. In the simplest estimate,  $\tau = -\ln(1 - T_b/T_d)$ . If we assume that the intrinsic dust temperature is in the range ( $90 < T_d \leq 180$  K), so as not to exceed the Arp 220 IRAS FIR luminosity, then  $\tau(1.3 \text{ mm}) \geq 0.7$ . This lower limit is already quite a “high”

opacity at 1.3 mm. Such a high-brightness dust source at 1.3 mm will certainly be opaque in the far-IR, so its intrinsic far-IR SED is simply a Planck curve. The spectrum deviates from a blackbody curve on the Wien side however, because it is attenuated by foreground dust. We observe deep CO(2–1) absorption due to foreground material, so this foreground attenuation must exist. The foreground dust is not as dense as the West-nucleus dust itself; it is optically thin at millimeter wavelengths, but optically thick in the mid-IR. Hence to fit the observed fluxes from the submillimeter through the mid-IR with a blackbody curve, we must first de-redden the observed mid-IR fluxes measured at the Keck telescope by Soifer et al. (1999). In a first iteration, we tried to match the luminosity of the West nucleus derived independently by Soifer et al. and Haas et al. (2001), and started with the foreground dust opacity ( $\tau = 1.2$  to 1.5) at  $25\mu\text{m}$  that Soifer et al. estimated by assuming the source size and dust temperature to be in the range from  $(0.39'', 102\text{ K})$  to  $(0.25'', 128\text{ K})$ . The source size that we measure, however, is even smaller,  $0.19'' \times 0.13''$ , implying a higher intrinsic dust temperature to reach the same luminosity, and hence a slightly higher foreground opacity to fit the mid-IR data points. Our current best compromise is shown in Fig. 5. This solution is for an intrinsic dust temperature of 170 K, a foreground dust opacity of  $\tau = 1.7$  at  $25\mu\text{m}$ , with a  $\lambda^{-1}$  opacity dependence at shorter wavelengths, and a  $\lambda^{-2}$  dependence at longer wavelengths.

In this solution, the Arp 220-West dust that we observe at millimeter wavelengths (not the foreground dust) has an optical depth of unity at 1.1 mm. For the observed source size, and an intrinsic dust temperature of 170 K, we obtain a total IR luminosity of  $9 \times 10^{11} L_{\odot}$  for the West nucleus. The dust flux implies a gas mass ( $\text{H}_2 + \text{He}$ ) of  $1 \times 10^9 M_{\odot}$ , and a mean  $\text{H}_2$  density of  $9 \times 10^4 \text{ cm}^{-3}$ , or  $5000 M_{\odot} \text{ pc}^{-3}$ . The mass could be lower if the dust grains are unusually large, and/or the abundances are super-solar. Such an enclosed mass yields, at radius 30 pc, a rotation velocity  $(GM/R)^{0.5}$  of  $370 \text{ km s}^{-1}$ , and this is about what we observe in CO. For this West dust source (not the foreground dust), if the optical depth scales as  $\lambda^{-2}$  to the mid-IR, then we expect  $\tau = 2000$  at  $25\mu\text{m}$ . If  $\tau \sim \lambda^{-1}$  from the mid-IR to the visible, then we expect  $\tau \approx 10^5$  at  $5000 \text{ \AA}$ .

What about the foreground dust? The observed CO absorption shows that the West dust core is also obscured by its surrounding, rapidly rotating West molecular disk, and possibly by some of the off-plane, larger-scale, Eastern disk material that may be in front of the West nucleus (see sketch by Mundell et al. 2001). This Eastern disk gas, that we modeled as a warped disk with a quasi polar-ring structure (Eckart & Downes 2001), is resolved, and therefore mostly absent in the long-baseline data presented here, but it may contribute to the absorption features that cut into the CO(2–1) line profiles from the West nucleus. For the values in our dust model shown in Fig. 5, the *observed* flux at  $25\mu\text{m}$  is 7.5 Jy (Soifer et al. 1999). The *intrinsic*, de-reddened dust flux at  $25\mu\text{m}$  is 42 Jy. The difference,

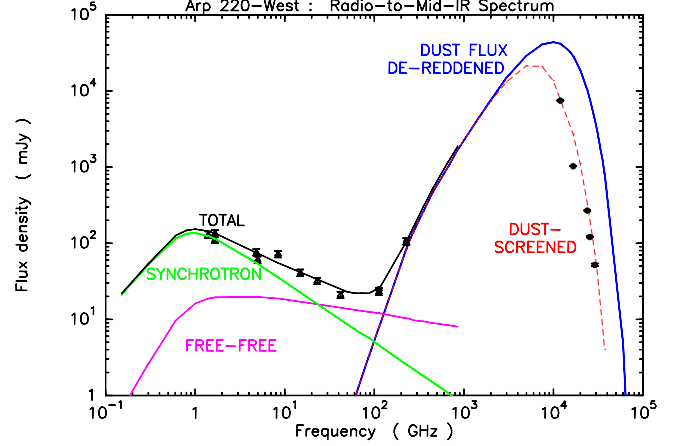


**Fig. 5.** Our model of the radio-to-mid-IR continuum spectrum of Arp 220-West. The spectrum is dominated by an opaque, 170 K blackbody dust component, with a luminosity of  $9 \times 10^{11} L_{\odot}$ , that only becomes optically thin below 1.1 mm. The dust blackbody is absorbed by a foreground screen (the West-CO ring and possibly part of the Eastern disk) that has a foreground opacity of 1.7 at  $25\mu\text{m}$ . The effect of the foreground screen is to attenuate the intrinsic mid-IR fluxes, thus shifting the apparent peak of the dust blackbody to longer wavelengths, giving the illusion of a lower temperature (dashed curve). Besides the millimeter-to-mid-IR dust component, there is a free-free component that becomes optically thick below 20 cm, and extended synchrotron emission mixed with the ionized gas, that turns over below 20 cm due to free-free absorption. The data points at 113 and 229 GHz are from this paper. The other radio fluxes are from the references cited in the text, and the mid-IR points are the 10 to  $25\mu\text{m}$  fluxes measured by Soifer et al. (1999).

due the foreground dust of the West molecular disk and possibly part of the Eastern disk, corresponds to a foreground opacity of 1.7 at  $25\mu\text{m}$ , close to the value of 1.5 estimated in one of the models by Soifer et al. It also implies a foreground opacity of  $\sim 20$  at  $K$  band, and a foreground  $A_V > 100$  in the visible, as previously inferred by Haas et al. (2001) from the weakness of the PAH feature. *This foreground extinction is why the Arp 220 has a cooler SED than the “warm”, AGN-powered ULIRGs* like Mrk 231 and the nearby quasars. At visible wavelengths, the AGN is hidden by  $10^4$  to  $10^5$  mag of obscuration by the dust torus, and this dust torus’s radiation is itself attenuated by an additional 100 mag due to the compact,  $0.5''$  West CO disk and possibly part of the larger-scale, warped Eastern CO disk.

#### 4. Conclusions

New CO(2–1) and 1.3 mm continuum data provide more evidence for a black hole in the Arp 220-West nucleus:

- 1) The Arp 220-West dust continuum has a *1.3 mm brightness temperature of 90 K*. This is much hotter than the dust detected at millimeter wavelengths from starburst

galaxies. SED fitting implies a dust opacity of unity at 1.1 mm, and a true dust temperature of 170 K, so the West disk strongly resembles that of the compact dust toroid around the quasar APM 08279+52 (Egami et al. 2000; Weiss et al. 2007).

2) The size of the West dust source is  $35 \times 20$  pc. This size and the 1.3 mm dust flux imply a gas density  $> 5000 M_{\odot} \text{pc}^3$ , about 10 times the stellar density in cores of giant ellipticals. Model SED fits that attempt to correct upward the mid-IR fluxes for attenuation by the foreground absorbing screen are consistent with a bolometric luminosity of  $9 \times 10^{11} L_{\odot}$ , that is, 75% of the total IRAS luminosity of Arp 220. Because of the foreground screen, the true *bolometric* luminosity is unknown; depending on geometry, it may be significantly higher than the IR luminosity derived from the IRAS data.

3) Strong CO absorption is seen in front of the dust continuum source. The inner dust source is a hot region, and is not the same source as the surrounding, cooler CO.

4) The West-CO torus centered on the compact 1.3 mm dust source has a steep velocity rise toward the nucleus, which is characteristic of a massive black hole (Fig. 3). The West molecular gas does not follow a rotation curve rising with radius, typical of inner-galaxy bulge regions. The CO must be rotating in the gravitational potential of a centrally-concentrated mass. The CO velocities in the West molecular torus extend to  $370 \text{ km s}^{-1}$  at a radius of 30 pc, which argues for an enclosed mass (gas + stars + black hole) of  $1 \times 10^9 M_{\odot}$ .

5) The data are consistent with the CO being in a cooler (50 K) ring surrounding a much hotter (170 K), dense dust source. The hot dust source is an inner, probably self-gravitating disk of radius 35 pc. The radio supernova candidates seen in VLBI maps extend over a slightly larger region, and some of them may be in the West CO torus rather than in the inner, opaque dust disk.

6) The combined proton column densities from the foreground main Arp 220 CO disk ( $10^3 \text{ cm}^{-3} \times 300 \text{ pc}$ ), plus the dense CO-West torus ( $10^4 \text{ cm}^{-3} \times 90 \text{ pc}$ ), plus the very dense, innermost dust disk ( $10^5 \text{ cm}^{-3} \times 30 \text{ pc}$ ) add up to  $\sim 1.3 \times 10^{25} \text{ cm}^{-3}$ . This is sufficient to hide all of the optical emission and most of the hard X-ray emission from the supermassive black hole accretion disk, which must be at the center of the  $0.19''$  continuum source seen at 1.3 mm.

7) **Why it is a black hole:** The dust source seen in these millimeter interferometer observations is small ( $0.19'' \times 0.13''$ ) and optically thick at 1.1 mm. Its black-body luminosity is nearly  $10^{12} L_{\odot}$ . The area of the dust disk on the sky is  $2 \times 10^3 \text{ pc}^2$ , so the emission surface brightness is  $\sim 5 \times 10^{14} L_{\odot} \text{ kpc}^{-2}$ . This puts impossible requirements on a starburst: the equivalent of 10 million O stars packed into the  $r = 35 \text{ pc}$  dust disk, with  $\sim 400$  O stars in each cubic parsec, or 30 times the luminosity of M82 from a thousand times smaller volume. No such super-starburst has ever been observed. This means the true source of the Arp 220-West luminosity cannot be a starburst. It can only be a black hole accretion disk.

*Acknowledgements.* We thank the Plateau de Bure Interferometer operators for their help with the observing, C. Thum, IRAM-Grenoble, for useful discussions, J. Conway, Onsala Space Observatory, for comments, and the referee for very helpful suggestions on improving the paper. IRAM is supported by INSU/CNRS (France), MPG (Germany) and IGN (Spain).

## References

- Anantharamaiah, K.R., Viallefond, F., Mohan, N.R., Goss, W.M., & Zhao, J.H. 2000, 537, 613
- Arribas, S., Colina, L., & Clements, D. 2001, ApJ, 560, 160
- Baan, W. & Haschick, A. 1995, ApJ, 454, 745 (BH95)
- Clements, D.L., McDowell, J.C., Shaked, S., Baker, A.C., Borne, K., Colina, L., Lamb, S.A., & Mundell, C. 2002, ApJ, 581, 974
- Colina, L., Arribas, S., & Clements, D., 2004, ApJ, 602, 181
- Downes, D., & Solomon, P.M. 1998, ApJ, 507, 615 (DS98)
- Eckart, A., & Downes, D. 2001, ApJ, 551, 730
- Egami, E., Neugebauer, G., Soifer, B.T., & Matthews, K. 2000, ApJ, 535, 561
- Fischer, J., Satyapal, S., Luhman, M.L., Melnick, G., Cox, P., Cernicharo, J., Stacey, G.J., Smith, H.A., Lord, S.D., & Greenhouse, M.A. 1997, in First ISO Workshop on Analytical Spectroscopy, ESA SP-419, ed. A. Heras et al., ESA, Noordwijk, p.149
- González-Alfonso, E., Smith, H.A., Fischer, J., & Cernicharo, J. 2004, ApJ, 613, 247
- Haas, M., Klaas, U., Müller, S.A.H., Chini, R., & Coulson, I. 2001, A&A, 367, L9
- Iwasawa, K., Sanders, D.B., Evans, A.S., Trentham, N., Miniutti, G., & Spoon, H.W.W. 2005, MNRAS, 357, 565
- Lonsdale, C.J., Diamond, P.J., Thrall, H., Smith, H.E., & Lonsdale, C.J. 2006, ApJ, 647, 185
- McDowell, J.C., Clements, D.L., Lamb, S.A., Shaked, S., Hearn, N.C., Colina, L., Mundell, C., Borne, K., Baker, A.C., & Arribas, S. 2003, ApJ, 591, 154
- Mundell, C.G., Ferruit, P., & Pedlar, A. 2001, ApJ, 560, 168
- Parra, R., Conway, J.E., Diamond, P.J., Thrall, H., Lonsdale, C.J., Lonsdale, C.J., & Smith, H.E. 2007, ApJ, 659, 314
- Ptak, A., Heckman, T., Levenson, N.A., Weaver, K., & Strickland, D. 2003, ApJ, 592, 782
- Rodríguez-Rico, C.A., Goss, W.M., Viallefond, F., Zhao, J.-H., Gómez, Y., & Anantharamaiah, K.R. 2005, ApJ, 633, 198
- Rovilos, E., Diamond, P.J., Lonsdale, C.J., Lonsdale, C.J., & Smith, H.E. 2003, MNRAS, 342, 373
- Rovilos, E., Diamond, P.J., Lonsdale, C.J., Smith, H.E., & Lonsdale, C.J. 2005, MNRAS, 359, 827
- Sakamoto, K., Scoville, N.Z., Yun, M.S., Crosas, M., Genzel, R., & Tacconi, L.J. 1999 ApJ, 514, 68
- Scoville, N.Z., Yun, M.S., & Bryant, P.M. 1997, ApJ, 484, 702
- Soifer, B.T., Neugebauer, G., Matthews, K., Becklin, E.E., Ressler, M., Werner, M.W., Weinberger, A.J., & Egami, E. 1999, ApJ, 513, 207
- Soifer, B.T., Neugebauer, G., Matthews, K., Egami, E., & Weinberger, A.J., 2002, AJ, 124, 2980
- Sopp, H., & Alexander, P. 1991, MNRAS, 251, 112
- Spoon, H.W.W., Moorwood, A.F.M., Lutz, D., Tielens, A.G.G.M., Siebenmorgen, R., & Keane, J.V. 2004, A&A, 414, 873
- Takano, S., Nakanishi, K., Nakai, N., & Takano, T. 2005, PASJ, 57, L29
- Weiss, A., Downes, D., Neri, R., Walter, F., Henkel, C., Wilner, D.J., Wagg, J., & Wiklind, T. 2007, A&A, 467, 955